Heliyon 10 (2024) e30105

Contents lists available at ScienceDirect

Heliyon

journal homepage: www.cell.com/heliyon

Research article

Hymenaea courbaril resin-mediated gold nanoparticles as catalysts in organic dyes degradation and sensors in pharmaceutical pollutants

Naeem Khan [a,*], Palwasha Durrani [a], Nargis Jamila [b,**], Umar Nishan [a], Muhammad Ishtiaq Jan [a], Riaz Ullah [c], Ahmed Bari [d], Ji Yeon Choi [e]

[a] Department of Chemistry, Kohat University of Science and Technology, Kohat, 26000, Khyber Pakhtunkhwa, Pakistan
[b] Department of Chemistry, Shaheed Benazir Bhutto Women University, Peshawar, 25000, Khyber Pakhtunkhwa, Pakistan
[c] Department of Pharmacognosy, College of Pharmacy, King Saud University, Riyadh, 11451, Saudi Arabia
[d] Department of Pharmaceutical Chemistry, College of Pharmacy, King Saud University, Riyadh, 11451, Saudi Arabia
[e] Food Analysis Research Center, Korea Food Research Institute, Wanju, 55365, Republic of Korea

ARTICLE INFO

Keywords:
Resin
Gold nanoparticles
Dyes
Degradation
Antibiotics
Sensing

ABSTRACT

In this study, green synthesis of gold nanoparticles (AuNPs) using aqueous extract from *Hymenaea courbaril* resin (HCR) is reported. The successful formation, functional group involvement, size, and morphology of the subject *H. courbaril* resin mediated gold nanoparticles (HCRAuNPs) were confirmed by Ultra Violet-Visible (UV–vis) spectroscopy, Fourier-Transform Infrared spectroscopy (FTIR), and Transmission Electron Microscopy (TEM) techniques. Stable and high yield of HCRAuNPs was formed in 1:15 (aqueous solution: salt solution) reacted in sunlight as indicated by the visual colour change and appearance of surface Plasmon resonance (SPR) at 560 nm. From the FT-IR results, the phenolic hydroxyl (–OH) functional group was found to be involved in synthesis and stabilization of nanoparticles. The TEM analysis showed that the particles are highly dispersed and spherical in shape with average size of 17.5 nm. The synthesized HCRAuNPs showed significant degradation potential against organic dyes, including methylene blue (MB, 85 %), methyl orange (MO, 90 %), congo red (CR, 83 %), and para nitrophenol (PNP, 76 %) up to 180 min. The nanoparticles also demonstrated the effective detection of pharmaceutical pollutants, including amoxicillin, levofloxacin, and azithromycin in aqueous environment as observable changes in color and UV–Vis spectral graph.

1. Introduction

Presently, the global community is grappling with severe environmental pollution manifesting in different types such as sound, air, thermal, soil, and noteworthy water pollution. The water contamination, a vital resource, is mainly attributed to dyes effluents added by industries like plastic, paper, textiles, chemicals, and pharmaceuticals. These effluents, loaded with nonbiodegradable toxic dyes, enter water resources, resulting to eutrophication and detrimentally disturbing aquatic life [1,2]. Furthermore, due to carcinogenic and mutagenic effect, these dyes have risks to human health and the broader ecosystem [3]. Plentiful initiatives and methodologies

* Corresponding author.
** Corresponding author.
E-mail addresses: naeem@kust.edu.pk (N. Khan), nargisjamila@sbbwu.edu.pk (N. Jamila).

https://doi.org/10.1016/j.heliyon.2024.e30105
Received 2 February 2024; Received in revised form 19 April 2024; Accepted 19 April 2024
Available online 20 April 2024

have been described in the literature to highlight this problem, with conventional water treatment techniques like chemical coagulation, activated carbon sorption, ultrafiltration, UV-light degradation, and electrochemical methods being generally employed for dye degradation [4]. However, these methods often exhibit toxicity, produce byproducts, expensive, and labor intensive. In response to environmental concerns, researchers have turned to alternative water treatment methods, with nano-catalysis emerging as a viable solution [5,6]. Notably, noble metal nanoparticles (NPs), owing to their large surface-to-volume ratio and finite size, have proven to be effective catalysts for dye degradation, with gold nanoparticles (AuNPs) being particularly favored due to their catalytic and opto-electrical properties, finding applications in diverse fields such as biosensors, optics, antibacterial agents, and anticancer agents [7–9].

Synthesis of AuNPs traditionally involves physical and chemical methods documented in the literature. Unfortunately, many of these methods employ toxic chemicals as starting materials, releasing hazardous by-products detrimental to human life and the ecosystem. Green route for AuNPs synthesis using plants, bacteria, fungi, macro algae (seaweeds), microalgae (cyanobacteria and diatoms) and their by-products (protein and lipids) have gained a great attention due to the reduced toxicity, biocompatibility, energy saving, non-toxic nature, managing climate change/global warning, environmental friendliness, and more sensible utilization of natural resources/agricultural waste [10–13]. Plants consist of bioactive phytochemicals (terpenoids, flavonoids, phenolics, tannins, essential oils), which reduce the metallic ions and result in NPs formation. Metal ions undergo oxidation or reduction during the process, depending on the biological media utilized [14]. The process begins with the nucleation of the metallic material and then progresses to the production of NPs within the mixture. According to literature, plant extracts are the superior biological media because they are more stable, decrease metal ions faster, and are simpler to scale up [15]. The phytochemicals containing functional groups such as hydroxyl (–OH), carbonyl (−), carboxyl (–COOH), aldehyde (–CHO), and oxygenated essential oils (EOs) play an important role in reducing and stabilizing NMs [16].

Due to widespread availability, low cost, environmental friendliness, plants are increasingly used for AuNPs synthesis. For example, Chidambaram et al. (2024) [17] utilized Abutilon theophrasti, Origanum majorana, Euphorbia hirta, and Senna auriculata for AuNPs synthesis. Similarly, various fruits and vegetables have also been reducing and stabilizing agents for AuNPs [18,19].

The precise and convenient detection of chemical and biological agents holds immense significance across diverse applications, encompassing fields like food and environmental monitoring, disease diagnostics, and forensics [20,21]. Among the array of detection techniques available, colorimetric sensors have garnered considerable attention due to their user-friendly nature, relatively straightforward design, and the ability to provide equipment-free readouts visible to the naked eye, rendering them particularly advantageous for on-site detection scenarios [22,23]. Nanomaterials (NMs) due to lower limits of detection and higher sensitivity are extensively used in sensing application. The covalent linkage of NMs to biomolecules enhances the sensing performance. AuNPs due to their light-scattering properties, strong optical absorption, unique chemical, biological, electronic properties, low or no toxicity, and fluorescence quenching has been widely used as sensors for optical recognition of antibiotics. Their unique optical properties are attributed to the mutual electronic oscillations at their surface, which can be easily shape up to the desired optical properties via controlling experimental parameters. Furthermore, AuNPs is also getting popular due to its simple preparation procedure [24]. To date, colorimetric assays based on AuNPs have been effectively employed for the detection of a wide spectrum of analytes, encompassing small molecules, nucleic acids, proteins, and metal ions [25–27].

Hymeneae courbrail L. belongs to the family Leguminosae and is distributed throughout the tropical and Himalaya region. Traditionally this plant is commonly used to cure pain, inflammation, headache, colds, and bronchitis [28]. *H. courbrail* L. resin extracts have been reported in literature for the presence of good concentrations of flavonoids, terpenes and coumarins [29]. Taking the vast medicinal applications and lack of nanostructural study on *H. courbrail* L. resin into consideration, the current study was aimed at synthesizing HCRAuNPs via green nanotechnology utilizing aqueous extract. The bio-based HCRAuNPs underwent comprehensive characterization through UV–Vis, FT-IR, and TEM experiments. The characterized AuNPs were then tested for their catalytic properties in dyes degradation and colorimetric sensing of selected antibiotics in water and biological samples including blood and urine.

2. Materials and methods

2.1. Selection of plant

H. courbaril resin (HCR) was collected in glass vials from Kohat, Khyber Pakhtunkhwa, Pakistan during flowering season, and refrigerated for use. The plant was identified by a taxonomist at the Department of Botany, Kohat University of Science and Technology, Kohat. It is a rich source of phenolic phytochemicals, which can be used as reducing and stabilizing agents in AuNPs synthesis.

2.2. Chemicals, reagents, and instrumentation

Analytical grade reagents, including gold chloride or chloroauric acid ($HAuCl_4.4H_2O$) were procured from Sigma Aldrich (Germany). The extracting solvents included ultrapure deionized water and ethanol. The dyes methylene blue, congo red, malachite green, para nitrophenol, and methyl orange were acquired from Merck (Germany). The antiseptic levofloxacin, amoxicillin and azithromycin were procured from Abbott (US). Deionized water was obtained from Q Millipore system. Confirmation of gold nanoparticles (AuNPs) synthesis was carried on Shimadzu UV–visible spectrophotometer (UV-1800). The HCRAuNPs were dispersed in deionized water using quartz cuvettes, and the instrument was calibrated using distilled water within the 200–800 nm range. Subsequently, alongside deionized water was employed as a reference. Functional groups in extracts involved in AuNPs synthesis were identified on Bruker FT-IR spectrometer within the range of 4000-400 cm^{-1}. Morphology and sizes of AuNPs were determined by FE-SEM (field emission-scanning electron microscope, Model 4800, Hitachi, Japan) and TEM (transmission electron microscopy, Phillips CM12,

Eindhoven, Netherlands) techniques. The operating procedures for SEM analysis were set as accelerating voltage (15 kV), magnification (x2.0 k),and working distance (7.7 mm). The TEM was operated at 120 kV. The samples were stained using uranyl acetate and sandwiched between two copper holders before being examined using a TEM microscope at various magnifications.

2.3. Extraction

To remove any dust and dirt, the resin was washed thoroughly with deionized water, dried in oven for 2 h at 60 °C. Then, it was finely chopped into fine powder. To prepare an aqueous extract, 10 g of HCR fine powder was dispersed in 100 mL deionized water. The mixture was filtered after being thoroughly heated for 2 h at 60 °C in a water bath.

2.4. Synthesis of HCRAuNPs

HCRAuNPs were synthesized by mixing different ratios (1:1, 1:2, 1:5, 1:10, 1:15, and 1:20) of gold salt solution (0.01 M) with 10 % resin solution [30]. Synthesis was carried out under several analytical parameters, including incubation, direct sunlight irradiation, stirring, and heating. The mixture color was noticed visually at time intervals (0–180 min), and then examined by electronic spectroscopy/UV–visible spectroscopy for appearance of SPR. The synthesized AuNPs were then separated by centrifugation at 10,000 rpm for about 15 min, washed, dried, and stored for further use.

2.5. Temperature and pH optimization for HCRAuNPs synthesis

In this study, AuNPs were synthesized and optimized for several factors such as ratios of HCR extract and gold salt solution, pH, temperature, and time for irradiation. The effect of temperature and pH on stability, physicochemical, and catalytic properties of HCRAuNPs has been studied according to previously published procedures [30]. The effect of temperature on AgNPs was studied in the range of 30–90^{o}C with an increment of 10^{o}C, and pH was adjusted from 2 to 12. pH was kept varied with hydrochloric acid (0.01 M) and sodium hydroxide (0.01 M) solutions. The changes in intrinsic SPR peak at various pH were recorded. The reaction mixtures were allowed to react in cuvette by shaking for 45–60 s, and then analyzed by UV–Vis spectroscopy.

2.6. Catalytic property of HCRAuNPs in dyes degradation

Catalytic potential of the synthesized HCRAuNPs in dyes degradation was determined using the established procedure previously published [31–33]. Briefly, 5.0 mg of synthesized HCRAuNPs were added to each dye solution (3.0 mL, 1.0 mM). The reaction mixtures were shaken for 2–3 min, and then exposed to direct sunshine. After 5.0 min of exposure to sunshine, the color change of each dye was recorded. Similarly, blank solutions were without the addition of HCRAuNPs and kept in direct sunshine. UV–visible spectra for these solutions were subsequently measured within 200–800 nm range. The percentage photocatalytic degradation was computed by the given equation (1).

$$\text{Degradation}\ (\%) = \frac{\text{A0} - \text{A}}{\text{A0}}\ \text{x}\ 100 \tag{1}$$

In the equation above, A0 is the absorption of dye solution and A is the absorption after degradation.

2.7. Sensing properties of HCRAuNPs in antibiotics detection

The antibiotics detection by HCRAuNPs in the current study was conducted by a procedure of Khan et al. (2023) [34]. In the procedure, working solutions (0.1 mM) of antibiotics were prepared in a suitable solvent (50 % ethanol). Each antibiotic solution (5.0 mL) was charged with 2.0 mg of HCRAuNPs and thoroughly shaken for 2–3 min. The control included the antibiotics solution only. After that, the UV–visible analysis of these reaction mixtures was conducted in range of 200–800 nm for 0–180 min. Furthermore, the linear ranges and limit of detection (LOD) of the HCRAuNPs were evaluated to determine the feasibility of detecting antibiotics. The limits of detection (LOD) were calculated as three times standard deviations (3xSD) from ten replicates of blank per slope of the calibration curve.

3. Results and discussion

3.1. Synthesis of gold nanoparticles

Under optimal conditions, resin-assisted HCRAuNPs were successfully synthesized. According to the results, HCR functioned both as a stabilizing and reducing agent in the synthesis of HCRAuNPs. The OH group in the constituents of resin is oxidized to carbonyl groups, reducing the gold ions (Au^{3+}) to elemental form (Au^{0}) as shown in the chemical equation (2) given below suggested by Kumar et al. (2021) [35].

$$Au^{3+} + \text{–CHO/}^{-}\text{OH} \rightarrow Au^{0} + \text{–COOH/C=O} \tag{2}$$

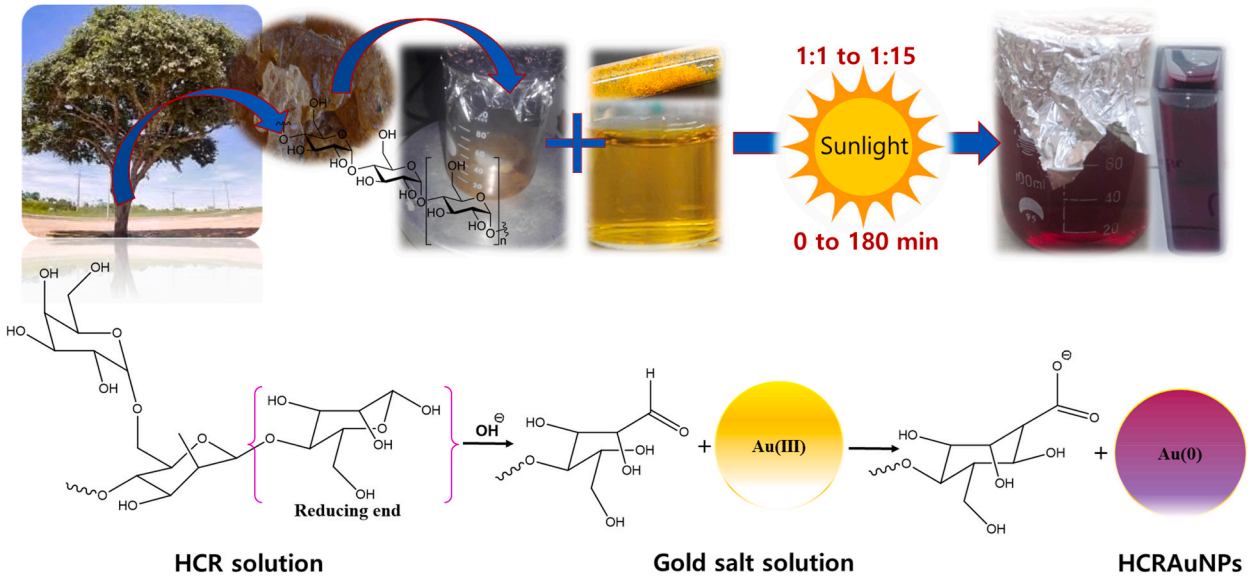

Fig. 1. Proposed reaction mechanism in HCRAuNPs synthesis.

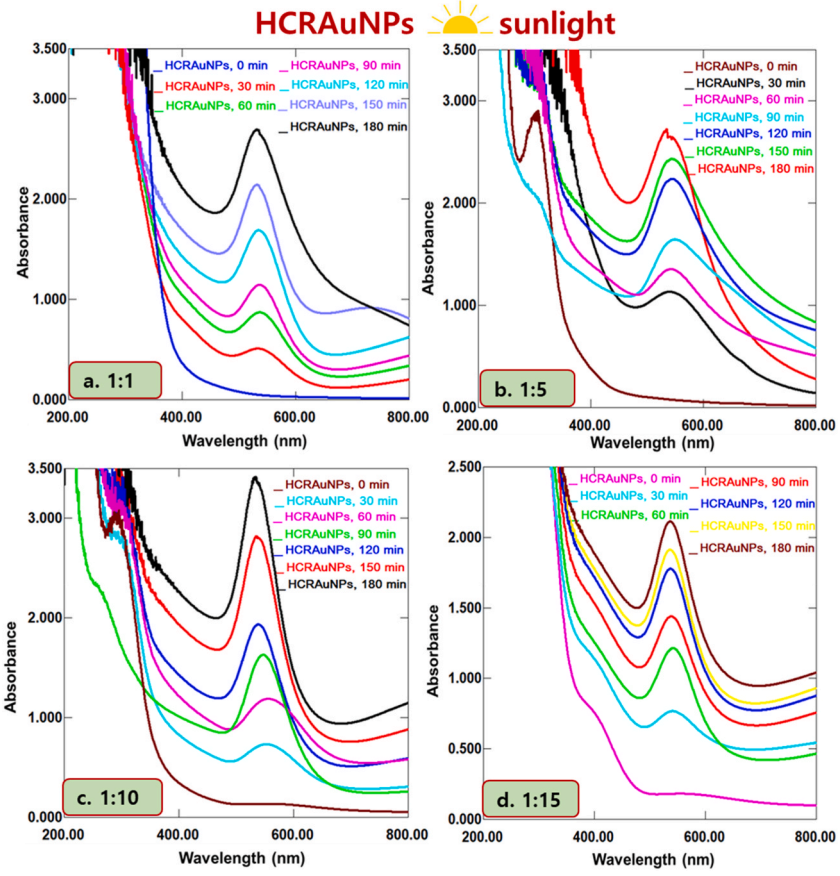

Fig. 2. Successive UV–Vis absorption spectra (200–800 nm) of HCRAuNPs synthesis based on composition ratio (a) 1:1, (b) 1:5, (c) 1:10, and (d) 1:15 of gold salt and HCR aqueous extract under sunlight. (For interpretation of the references to color in this figure legend, the reader is referred to the Web version of this article.)

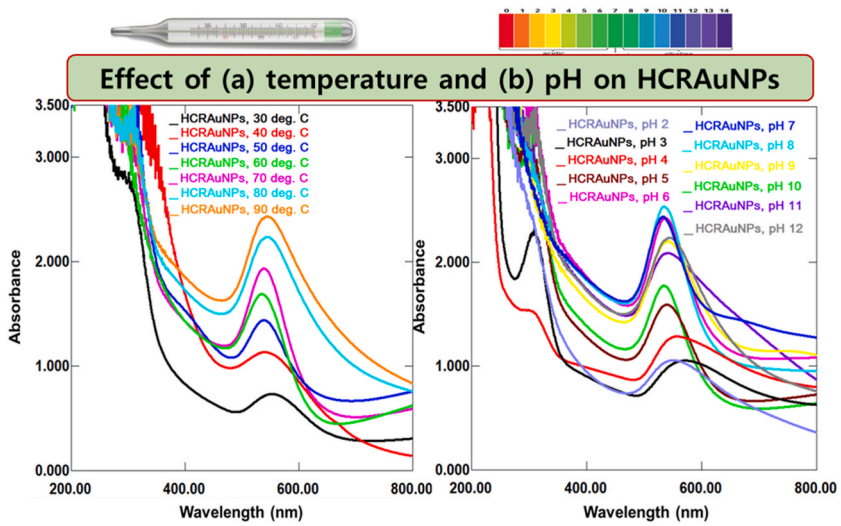

Fig. 3. Successive UV–Vis absorption spectra showing effect of (a) temperature and (b) pH on synthesized HCRAuNPs.

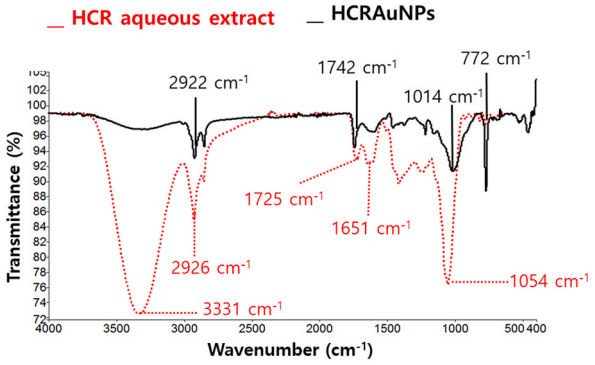

Fig. 4. FT-IR spectra of HCR aqueous extract and HCR aqueous extract mediated HCRAuNPs.

Another study by Tagad et al. (2014) [36] concluded that the hydroxyl groups (OH) and the hemiacetal (RHC(OH)OR) reducing ends of the gum/resin are the active reaction centers/points, which facilitate Au(III) to Au(0) as shown in Fig. 1.

In the current study, the AuNPs synthesis was examined under various physical parameters. The color change, followed by electronic/UV–Vis spectroscopy, FTIR, SEM, and TEM analysis, validated the synthesis of nanoparticles. The provided ratios (1:1, 1:2, 1:5, 1:10, 1:15 and 1:20) of aqueous solution of HCR and gold chloride salt indicated successful formation of HCRAuNPs under direct sunshine. Preliminarily, the synthesis was confirmed by colour change from yellow to ruby red/purple and then by the appearance of SPR band at 520-60 nm range in the UV–visible spectroscopy. The spectral graph (Fig. 2a–d) displaying a characteristic SPR absorption at 560 nm confirmed HCRAuNPs formation. The UV–visible spectra (Fig. 2d) indicated that among the ratios of 1:1. 1:5, 1:10, and 1:15, sunlight at a ratio of 1:15 resulted in the formation of the most stable and high yield HCRAuNPs as indicated by the intensity of absorption peak at 550–560 nm [37]. Similarly, the distinctive peak intensity and position in response to time and direct sun irradiation revealed a high concentration of HCRAuNPs for 180 min, which could be considered an ideal time for HCRAuNP synthesis. Moreover, by increasing the time beyond 180 min and the ratio (>1:15), a wider SPR band towards red shift and turbidity was observed in the AuNPs dispersion, which indicates the agglomeration beyond these parameters [38].

3.2. *Effect of temperature and pH on HCRAuNPs synthesis and stability*

The temperature influence on the synthesis of HCRAuNPs can be observed in the UV–visible spectra (Fig. 3a). The intensity of the distinctive SPR peak increased with increasing temperature. The position and strength of different SPR peaks indicate that stable HCRAuNPs synthesis occurred at 60 °C. The shift and broadening of characteristic peaks with increasing temperature revealed that these nanoparticles (NPs) are unstable and agglomerated. Under sunlight, 60 °C was found to be ideal temperature for the synthesis of HCRAuNPs.

On the other hand, the pH effect on the formation of HCRAuNPs indicated that at 1:15 ratio in sunlight irradiation, a 7.5 is appeared

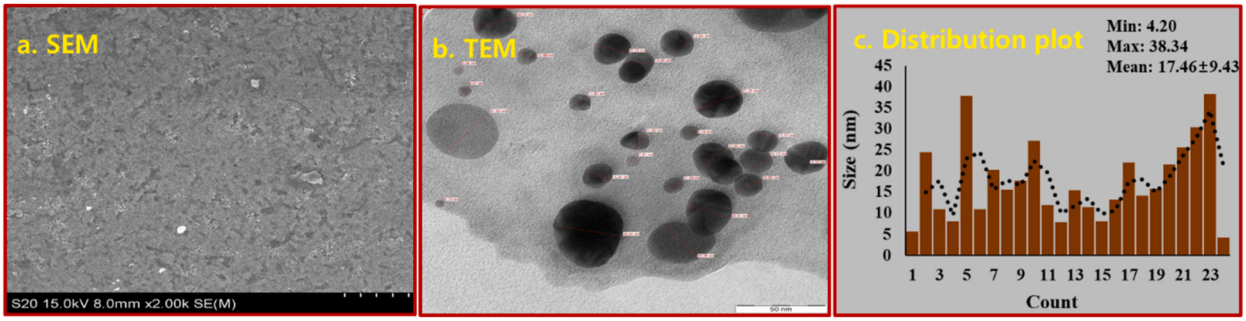

Fig. 5. Size/surface morphology of HCRAuNPs by (a) SEM, (b) TEM, and (c) histogram distribution plot.

to be the best pH for the subject AuNPs synthesis as demonstrated by a very sharp SPR peak (Fig. 3b). The higher pH (8–10) suggested that the reactants are rapidly used in precipitation. Furthermore, the pH has a considerable influence on the morphology and size of AuNPs, since quick salt reduction and uniform nucleation at high optimal pH leads to good AuNPs formation [39].

3.3. Characterization of synthesized HCRAuNPs

The synthesized HCRAuNPs were subjected to various analyses such as FT-IR for the determination of presence and involvement of the functional groups in AuNPs synthesis, and TEM for size and morphology determination.

3.3.1. Characterization by FT-IR spectroscopy

The FT-IR analysis of HCR and HCRAuNPs was recorded to identify the possible functional groups present in the phytochemicals of HCR, which are responsible for the reduction of gold ions (Au^{3+}) and stabilizing the reduced HCRAuNPs. The FTIR spectra of HCR showed characteristic broad band for OH stretching vibration at 3331 cm^{-1} (Fig. 4). C═O stretching vibration was observed at a frequency of 1725 cm^{-1}. Bands at 2926/2922 cm^{-1} indicate the aliphatic –C-H stretching vibrations [40]. In case of HCRAuNPs, the characteristic stretching vibration band of OH stretching vibration is shifted toward lower/decreased/disappeared frequency (Fig. 4). The shift of OH and CO bands in HCRAuNPs spectra demonstrated that OH group is actively involved in AuNPs synthesis. The OH groups of the sugar units (polysaccharides) are assumed to be active in the reduction and stability of HCRAuNPs, as demonstrated by comparative study of the FTIR spectra. The reduction of Au(III) to Au(0) by OH group and the hemiacetal (RHC(OH)OR) reducing ends of the gum/resin is further confirmed by an appearance of absorption peak at 1752 cm^{-1} which is assigned to the carboxyl group formed by the oxidation of hemiacetal/aldehyde groups) upon the addition of Au^{3+} ions [36]. The results of the FTIR analysis of HCR and HCRAuNPs revealed that an organic layer from the HCR aqueous solution is formed around the HCRAuNPs, and the reduction of Au^{3+} to Au^{0} is attributed to be carried out by the polysaccharides present in HCR [41].

3.3.2. Characterization by SEM and TEM

To determine the size and shape of HCRAuNPs, SEM and TEM analyses were conducted. The SEM image (Fig. 5a) demonstrated spherical shapes with some rectangle-shaped particles in them. TEM image (Fig. 5b) demonstrated that the average size of HCRAuNPs is 17.5 nm, as revealed from the histogram distribution plot (Fig. 5c).

3.4. Dyes degradation by HCR-AuNPs

Photocatalytic activity of the NPs is to create an electron–hole pair by exposure to solar radiation. This activity of NPs has potential use in sterilization, sanitation, and wastewater remediation as anti-soiling, antifungal, anti-bacterial, and antiviral agent under exposure to solar/visible/ultraviolet light. Kumar et al. (2021) [35] suggests that in photocatalysis, the excitons formed react with the exciton trapping molecules adsorbed on the surface of catalyst forming free radicals, which in turn react with the organic dye molecules. In this process, the electrons of nanocatalyst excite by absorbing photons from valence band to conduction band, thus, generating electron (e−)/hole (h+) pairs. The holes react with water (H_2O) molecules as well as with the surface-adsorbed hydroxide ions, forming hydroxyl radical (•OH) and hydronium ions (H+). Then, the •OH radicals absorbed on the surface of the catalyst oxidize the dye to small inorganic molecules. The photocatalytic degradation mechanism of MNPs is represented by the following reactions (3–9) outlined by Kumar et al. (2021) in his publication.

$$\mathrm{MNPs} + h\nu \rightarrow h^{+} + e^{-} \text{ (photo generation of excitons)} \quad (3)$$

$$\mathrm{H_2O} + h^{+} \rightarrow \bullet OH + H^{+} \quad (4)$$

$$OH^{-} + h^{+} \rightarrow {}^{\bullet}OH \quad e^{-} + O_2 \rightarrow {}^{\bullet}O_2 \quad (5)$$

$$^{\bullet}O_2H + H^{+} \rightarrow {}^{\bullet}OOH/H_2 \quad (6)$$

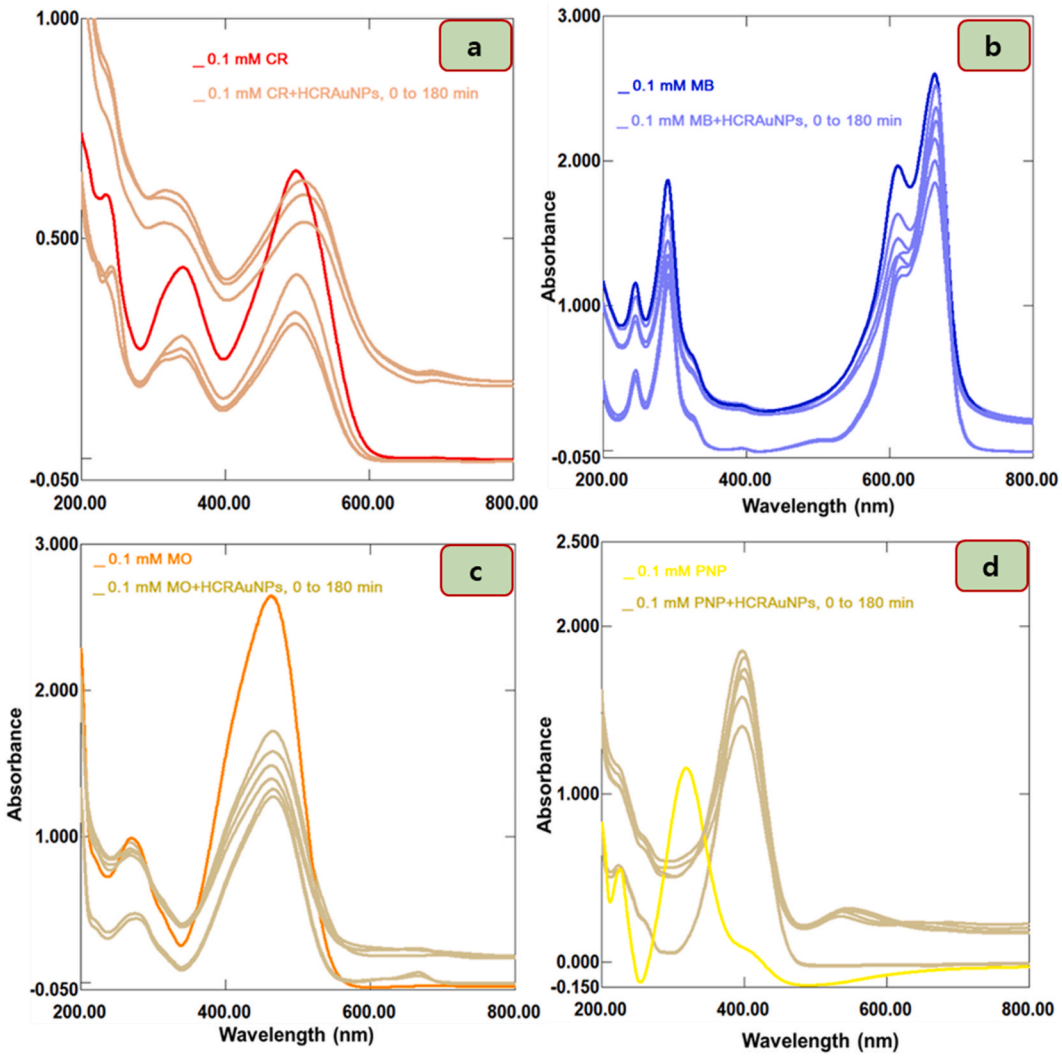

Fig. 6. Successive UV–Vis absorption spectra dyes degradation (a) CR, (b) MB, (c) MO, and (d) PNP by HCRAuNPs.

$$\frac{\text{Θ}}{2} \rightarrow \bullet OH + \bullet OH \tag{7}$$

$$\text{Dye} + h\nu \rightarrow \text{Dye}^* \tag{8}$$

$$\text{Dye}^* + O_2 \text{ or } \bullet OH \text{ or } \bullet O_2^- \rightarrow (\text{unstable intermediate}) \rightarrow \text{degradation products } (CO_2 + H_2O) \tag{9}$$

In the study, the synthesized HCRAuNPs were analyzed for their catalytic activity in dyes degradation. The toxic dyes, MB, MO, CR, and PNP were significantly degraded as depicted in Fig. 6a–d. In the absence of HCRAuNPs, these dyes showed stability under sunlight irradiation. However, in the presence of HCRAuNPs, the dyes degraded significantly, which suggests the photo catalytic potential of the subject NPs. At zero time (t_0), the decrease in absorption intensity of dyes at their characteristic wavelength demonstrated the attachment of dyes over the surface of NPs. The provided UV–visible spectra (Fig. 6a–d) showed that HCRAuNPs successfully degraded the dyes for up to 180 min. Furthermore, the irregularity in UV–visible spectral λ_{max} of the test dyes up to 10 min indicated the spread and interaction over the surface of HCRAuNPs. The HCRAuNPs showed the highest degradation potential for MO with 90 % degradation. Similarly, MB and RhB were significantly degraded, with 85 % and 83 % degradation. The percentage degradation of CR and PNP was 68 % and 76 %. The provided data revealed that the synthesized HCRAuNPs have significant degradation potential and lower activation energy.

3.5. Sensing of antibiotics (pharmaceutical pollutants) by HCRAuNPs

The synthesized HCRAuNPs were used for colorimetric sensing of broad-spectrum antibiotics including levofloxacin, amoxicillin, and azithromycin. A 1.0 mg HCRAuNPs was added to 3 mL (0.1 mM solution) of antibiotics. The optimal conditions for sensing of these antibiotics are found to be (35 °C, 15 min, and pH 7). The comparative UV–visible spectra (Fig. 7) revealed high sensitivity and

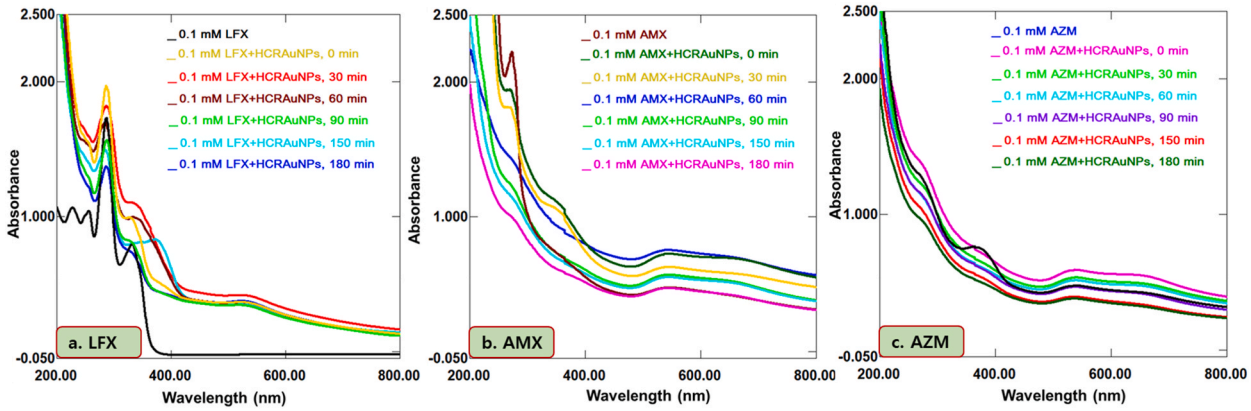

Fig. 7. Successive UV–Vis absorption spectra of antibiotics (a) LFX, (b) AMX, and (c) AZM by HCRAuNPs.

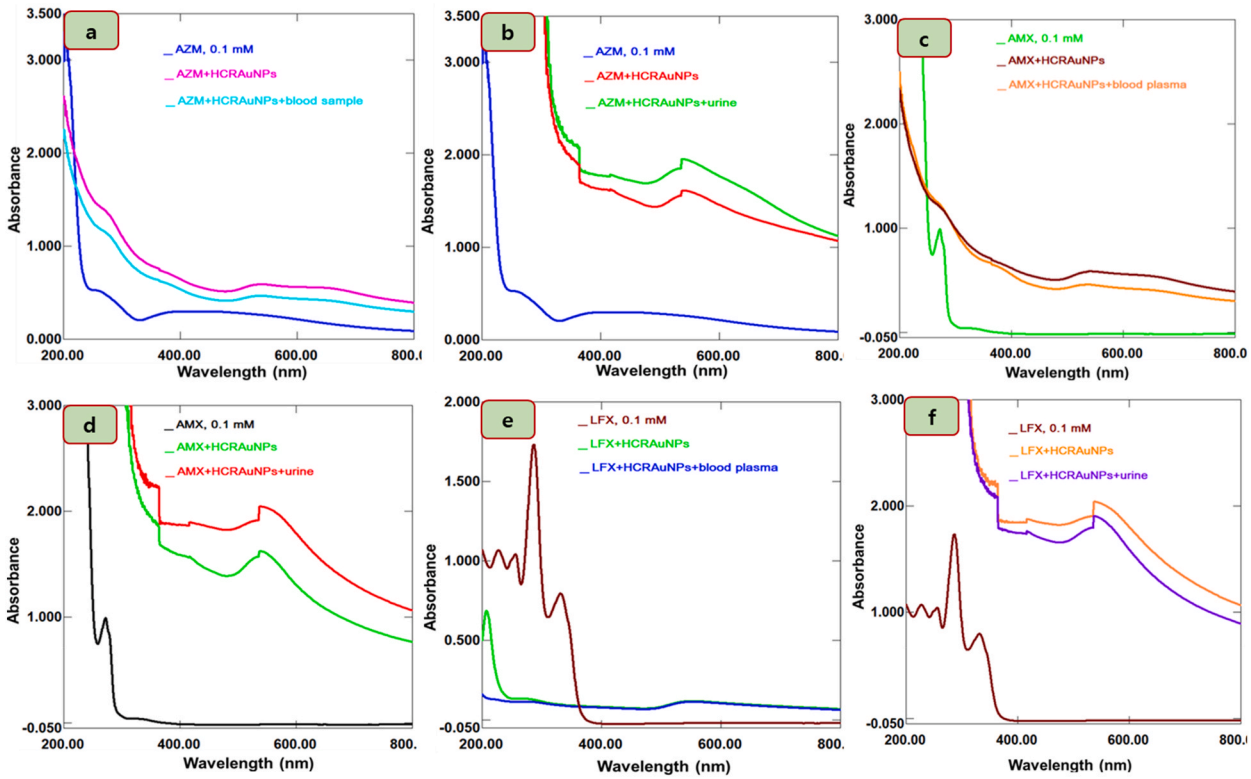

Fig. 8. Successive UV–Vis absorption spectra showing (a & b) AZM, (c & d) AMX, and (e & f) LFX antibiotics sensing by HCRAuNPs in blood plasma and urine samples, respectively.

specificity of the synthesized HCRAuNPs in antibiotic detection. LFX (Fig. 7a) exhibits an absorption peak at λ_{max} 288 nm. Upon the addition of HCRAuNPs, this λ_{max} gets reduced. Similarly, AMX (Fig. 7b) having an absorption maximum at λ_{max} 229 nm and 278 nm, and AZM (Fig. 7c) at λ_{max} 212 nm and 367 nm, lead to reduction with time interval upon HCRAuNPs addition. This decrease in λ_{max} of respective antibiotics is due to decrease in the concentration via their adsorption on HCRAuNPs surface. The antibiotics were also significantly detected in real samples, including blood plasma and urine collected from patients provided with these antibiotics. Furthermore, Fig. 8a-f depicts the results of antibiotics (AZM, AMX, and LFX) detection by HCRAuNPs in blood plasma and urine samples. Because of the hydrogen-bonding interaction, the synthesized HCRAuNPs showed a high affinity for antibiotics. Inter-particle cross-linking of AuNPs occurs as a result, leading to naked color shifts as shown by UV–visible spectra. Different classes of antibiotics adsorb on NPs with different potential due to the differences in their dispersibility, temperature, pH, class and volume, and hence, remove with different extent. Previous reports revealed that NPs due to different functional groups from various phytoconstituents on their surfaces possess some negatively charged ions. The antibiotic molecules are positively charged, which leads to the cation-

Table 1
Linear ranges and limits of detection (LOD) in antibiotics sensing by HCRAuNPs.

Antibiotic molecule	Linear range (mM)	LOD (mM)
AMX	0.02–0.24	0.015
LFX	0.03–0.21	0.012
AZM	0.03–0.18	0.013

exchange or π–π interaction mechanism with NPs, and ultimately increase their adsorption on the surface of NPs [42]. In the detection performance of the HCRAuNPs in antibiotics detection, the linear ranges and the LOD found are listed in Table 1. The minimum detection limit was exhibited for LFX followed by AZM. These results are in good agreement to several previous literature [43,44].

4. Conclusions

In the current research study, the successful synthesis of gold nanoparticles utilizing a novel *H. courbaril* resin has been achieved. The optimal synthesis of HCRAuNPs was achieved using an aqueous solution of HCR and gold salt in 1:15 under direct sunlight irradiation, which proved to be an inexpensive, straightforward, and environment friendly method. Comprehensive characterizations confirmed the spherical nature of the synthesized HCRAuNPs. Infrared spectroscopy indicates the presence of polysaccharides and phenolic compounds in the HCR extract, which is responsible for the reduction of gold salt (Au^{3+}) to Au^0. However, other phytochemicals present in HCR likely act as capping agents, preventing agglomeration. Transmission electron micrograph revealed the spherical morphology of the synthesized HCRAuNPs with an average size of 17.5 nm. Furthermore, the photocatalytic degradation of dyes using the synthesized HCRAuNPs as a catalyst was conducted. The synthesized HCRAuNPs exhibited remarkable efficacy with substantial percentage degradation (reaching up to 90 %) in the degradation of methylene blue, methyl orange, congo red, and paranitrophenol. Moreover, the synthesized HCRAuNPs demonstrated promising colourimetric sensing capabilities against selected antibiotics: amoxicillin, azithromycin, and levofloxacin. Consequently, prepared HCRAuNPs hold significant potential for commercial applications in dye degradation and antibiotic sensing.

Statements and declarations

Authors confirm that the manuscript has been read and approved by all named authors and that there are no other people who satisfied the criteria for authorship but are not listed. It is further confirmed that the order of authors listed in the manuscript has been approved by all authors. The corresponding author on behalf of all authors of the manuscript further declares that there is no any potential competing interests.

Data availability statement

The authors confirm that the data supporting the findings of this study are available within the article and its supplementary materials. However, the raw data will be available upon request from the corresponding author.

CRediT authorship contribution statement

Naeem Khan: Writing – review & editing, Writing – original draft, Supervision, Project administration, Methodology, Conceptualization. **Palwasha Durrani:** Investigation, Formal analysis. **Nargis Jamila:** Methodology, Funding acquisition, Conceptualization. **Umar Nishan:** Writing – review & editing, Writing – original draft, Validation, Investigation. **Muhammad Ishtiaq Jan:** Writing – review & editing, Writing – original draft, Validation, Resources, Investigation. **Riaz Ullah:** Writing – review & editing, Writing – original draft, Validation, Investigation, Funding acquisition. **Ahmed Bari:** Writing – review & editing, Writing – original draft, Funding acquisition. **Ji Yeon Choi:** Writing – review & editing, Writing – original draft, Validation, Resources, Investigation.

Declaration of competing interest

The authors declare that they have no known competing financial interests or personal relationships that could have appeared to influence the work reported in this paper.

Acknowledgements

Authors wish to thank Researchers Supporting Project Number (RSP2024R346) at King Saud University Riyadh Saudi Arabia for financial support.

References

[1] P. Srivatsav, B.S. Bhargav, V. Shanmugasundaram, J. Arun, K.P. Gopinath, A. Bhatnagar, Biochar as an eco-friendly and economical adsorbent for the removal of colorants (dyes) from aqueous environment: a review, Water 12 (2020) 3561, https://doi.org/10.3390/w12123561.

[2] M. Bashir, M. Batool, N. Arif, M. Tayyab, Y.-J. Zeng, M.N. Zafar, Strontium-based nanomaterials for the removal of organic/inorganic contaminants from water: a review, Coord. Chem. Rev. 492 (2023) 215286, https://doi.org/10.1016/j.ccr.2023.215286.

[3] J. Lin, W. Ye, M. Xie, D.H. Seo, J. Luo, Y. Wan, B. Van der Bruggen, Environmental impacts and remediation of dye-containing wastewater, Nat. Rev. Earth Environ. 4 (2023) 785–803, https://doi.org/10.1038/s43017-023-00489-8.

[4] M.D. Khan, A. Singh, M.Z. Khan, S. Tabraiz, J. Sheikh, Current perspectives, recent advancements, and efficiencies of various dye-containing wastewater treatment technologies, J. Water Process Eng. 53 (2023) 103579, https://doi.org/10.1016/j.jwpe.2023.103579.

[5] A. Akbari, Z. Sabouri, H.A. Hosseini, A. Hashemzadeh, M. Khatami, M. Darroudi, Effect of nickel oxide nanoparticles as a photocatalyst in dyes degradation and evaluation of effective parameters in their removal from aqueous environments, Inorg. Chem. Commun. (2020) 107867, https://doi.org/10.1016/j.inoche.2020.107867.

[6] G. Bhavya, S.A. Belorkar, R. Mythili, N. Geetha, H.S. Shetty, S.S. Udikeri, S. Jogaiah, Remediation of emerging environmental pollutants: a review based on advances in the uses of eco-friendly biofabricated nanomaterials, Chemosphere 275 (2021) 129975, https://doi.org/10.1016/j.chemosphere.2021.129975.

[7] H. Sheng, J. Wang, J. Huang, Z. Li, G. Ren, L. Zhang, L. Yu, M. Zhao, X. Li, G. Li, Strong synergy between gold nanoparticles and cobalt porphyrin induces highly efficient photocatalytic hydrogen evolution, Nat. Commun. 14 (2023) 1528, https://doi.org/10.1016/j.chemosphere.2021.129975.

[8] R. Sanchis-Gual, M. Coronado-Puchau, T. Mallah, E. Coronado, Hybrid nanostructures based on gold nanoparticles and functional coordination polymers: chemistry, physics and applications in biomedicine, catalysis and magnetism, Coord. Chem. Rev. 480 (2023) 215025, https://doi.org/10.1016/j.ccr.2023.215025.

[9] M.A. Sobi, D. Usha, R. Rajagopal, S. Arokiyaraj, M. Bindhu, Phytosynthesizing gold nanoparticles: characterization, bioactivity, and catalysis evaluation, J. Mol. Struct. 1302 (2024) 137308, https://doi.org/10.1016/j.molstruc.2023.137308.

[10] B. Ahmed, M.B. Tahir, M. Sagir, M. Hassan, Bio-inspired sustainable synthesis of silver nanoparticles as next generation of nanoproduct in antimicrobial and catalytic applications, Mater. Sci. Eng. B 301 (2024) 117165, https://doi.org/10.1016/j.mseb.2023.117165.

[11] G.A. Vinnacombe-Willson, Y. Conti, A. Stefancu, P.S. Weiss, E. Cortés, L. Scarabelli, Direct bottom-up in situ growth: a paradigm shift for studies in wet-chemical synthesis of gold nanoparticles, Chem. Rev. 13 (2023) 8488–8529, https://doi.org/10.1021/acs.chemrev.2c00914.

[12] S. Kumari, S. Raturi, S. Kulshrestha, K. Chauhan, S. Dhingra, K. András, K. Thu, R. Khargotra, T. Singh, A comprehensive review on various techniques used for synthesizing nanoparticles, J. Mater. Res. Technol. 27 (2023) 1739–1763, https://doi.org/10.1016/j.jmrt.2023.09.291.

[13] M.M. El-Sheekh, H.H. Morsi, L.H. Hassan, S.S. Ali, The efficient role of algae as green factories for nanotechnology and their vital applications, Microbiol. Res. 263 (2022) 127111, https://doi.org/10.1016/j.micres.2022.127111.

[14] S. Antunes Filho, M.S. Dos Santos, O.A.L. Dos Santos, B.P. Backx, M.L. Soran, O. Opriş, I. Lung, A. Stegarescu, M. Bououdina, Biosynthesis of nanoparticles using plant extracts and essential oils, Molecules 28 (2023) 3060, https://doi.org/10.3390/molecules28073060.

[15] A. Nyabadza, E. McCarthy, M. Makhesana, S. Heidarinassab, A. Plouze, M. Vazquez, D. Brabazon, A review of physical, chemical and biological synthesis methods of bimetallic nanoparticles and applications in sensing, water treatment, biomedicine, catalysis and hydrogen storage, Adv. Colloid Interface Sci. 321 (2023) 103010, https://doi.org/10.1016/j.cis.2023.103010.

[16] D. Patra, R. El Kurdi, Curcumin as a novel reducing and stabilizing agent for the green synthesis of metallic nanoparticles, Green Chem. Lett. Rev. 14 (2021) 474–487, https://doi.org/10.1080/17518253.2021.1941306.

[17] J. Chidambaram, P. Upadhyay, D. Sahal, K. Chinnaperumal, T. Rajendran, S. Durairaj, D. Saravanan, R.M. Rathinasamy, Biosynthesis of gold nanoparticles mediated by medicinal phytometabolites: an effective tool against plasmodium falciparum and human breast cancer cells, J. Drug Deliv. Sci. Technol. (2024) 105520, https://doi.org/10.1016/j.jddst.2024.105520.

[18] T.P. Patil, A.A. Vibhute, S.L. Patil, T.D. Dongale, A.P. Tiwari, Green synthesis of gold nanoparticles via Capsicum annum fruit extract: characterization, antiangiogenic, antioxidant and anti-inflammatory activities, Appl. Surf. Sci. Adv 13 (2023) 100372, https://doi.org/10.1016/j.jddst.2024.105520.

[19] H. Park, W. Kim, M. Kim, G. Lee, W. Lee, J. Park, Eco-friendly and enhanced colorimetric detection of aluminum ions using pectin-rich apple extract-based gold nanoparticles, Spectrochim. Acta A Mol. Biomol. Spectros. 245 (2021) 118880, https://doi.org/10.1016/j.saa.2020.118880.

[20] U.S. Kadam, J.C. Hong, Recent advances in aptameric biosensors designed to detect toxic contaminants from food, water, human fluids, and the environment, Trends Environ. Anal. Chem. 36 (2022) e00184, https://doi.org/10.1016/j.teac.2022.e00184.

[21] Z. Sadiq, S.H. Safiabadi Tali, H. Hajimiri, M. Al-Kassawneh, S. Jahanshahi-Anbuhi, Gold nanoparticles-based colorimetric assays for environmental monitoring and food safety evaluation, Crit. Rev. Anal. Chem. (2022) 1–36, https://doi.org/10.1080/10408347.2022.2162331.

[22] R. Umapathi, S. Sonwal, M.J. Lee, G.M. Rani, E.-S. Lee, T.-J. Jeon, S.-M. Kang, M.-H. Oh, Y.S. Huh, Colorimetric based on-site sensing strategies for the rapid detection of pesticides in agricultural foods: new horizons, perspectives, and challenges, Coord. Chem. Rev. 446 (2021) 214061, https://doi.org/10.1016/j.ccr.2021.214061.

[23] J. Zhou, Y. Liu, X. Du, Y. Gui, J. He, F. Xie, J. Cai, Recent advances in design and application of nanomaterials-based colorimetric biosensors for agri-food safety analysis, ACS Omega 8 (2023) 46346–46361, https://doi.org/10.1021/acsomega.3c06409.

[24] Q.U.A. Zahra, Z. Luo, R. Ali, M.I. Khan, F. Li, B. Qiu, Advances in gold nanoparticles-based colorimetric aptasensors for the detection of antibiotics: an overview of the past decade, Nanomaterials 11 (2021) 840, https://doi.org/10.3390/nano11040840.

[25] Y. Geng, W.J. Peveler, V.M. Rotello, Array-based “Chemical Nose” sensing in diagnostics and drug discovery, Angew. Chem. 58 (2019) 5190–5200, https://doi.org/10.1002/anie.201809607.

[26] H. Duan, Y. Wang, S.-Y. Tang, T.-H. Xiao, K. Goda, M. Li, A CRISPR-CAS1 2a powered electrochemical sensor based on gold nanoparticles and mxene composite for enhanced nucleic acid detection, Sensor. Actuator. B Chem. 380 (2023) 133342, https://doi.org/10.1016/j.snb.2023.133342.

[27] E.-S. Lee, E.-J. Kim, T.-K. Park, D.-W. Bae, S.-S. Cha, T.-W. Kim, Y.-P. Kim, Gold nanoparticle-assisted selex as a visual monitoring platform for the development of small molecule-binding DNA aptasensors, Biosens. Bioelectron. 191 (2021) 113468, https://doi.org/10.1016/j.bios.2021.113468.

[28] V.E. McCoy, A. Boom, M.M.S. Kraemer, S.E. Gabbott, The chemistry of American and African amber, copal, and resin from the genus *Hymenaea*, Org. Geochem. 113 (54) 43-54. https://www.sciencedirect.com/science/article/pii/S0146638017301857.

[29] J. Anaya-Gil, P. Ramos-Morales, A. Muñoz-Hernandez, A. Bermúdez, H. Gomez-Estrada, In vivo evaluation of the toxic activity and genotoxicity of the *Hymenaea courbaril* L.’s resin in *Drosophila melanogaster*, Saudi J. Biol. Sci. 29 (2022) 480–488, https://doi.org/10.1016/j.sjbs.2021.09.005.

[30] N. Jamila, N. Khan, N. Bibi, M. Waqas, S.N. Khan, A. Atlas, F. Amin, F. Khan, M. Saba, Hg (II) sensing, catalytic, antioxidant, antimicrobial, and anticancer potential of *Garcinia mangostana* and α-mangostin mediated silver nanoparticles, Chemosphere 272 (2021) 129794, https://doi.org/10.1016/j.chemosphere.2021.129794.

[31] N. Jamila, N. Khan, A. Bibi, A. Haider, S.N. Khan, A. Atlas, U. Nishan, A. Minhaz, F. Javed, A. Bibi, *Piper longum* catkin extract mediated synthesis of Ag, Cu, and Ni nanoparticles and their applications as biological and environmental remediation agents, Arab. J. Chem. 13 (2020) 6425–6436, https://doi.org/10.1016/j.arabjc.2020.06.001.

[32] M. Saba, F. Khitab, N. Jamila, N. Khan, F. Amin, N. Bibi, R.A. Qazi, S.N. Khan, Gold nanoparticles from *Chenopodium botrys* and *Chenopodium ambrosioides* as bioreductants: *In vitro* antioxidant, antibacterial, and an eco-friendly catalytic potential in dyes degradation, Arabian J. Sci. Eng. 49 (2024) 685–697, https://doi.org/10.1007/s13369-023-08382-8.

[33] M. Mehta, M. Sharma, K. Pathania, P.K. Jena, I. Bhushan, Degradation of synthetic dyes using nanoparticles: a mini-review, Environ. Sci. Pollut. Res. 28 (2021) 49434–49446, https://doi.org/10.1007/s11356-021-15470-5.

[34] N. Khan, F. Kalsoom, N. Jamila, S. Shujah, A.U.H.A. Shah, U. Nishan, M.I. Jan, I.M. Hwang, M.S. Elshikh, R. Ullah, *Micromeria biflora* mediated gold and silver nanoparticles for colourimetric detection of antibiotics and dyes degradation, J. King Saud Univ. Sci. 35 (2023) 102999, https://doi.org/10.1016/j.jksus.2023.102999.

[35] B. Kumar, Green synthesis of gold, silver, and iron nanoparticles for the degradation of organic pollutants in wastewater, J. Compos. Sci. 5 (2021) 219, https://doi.org/10.3390/jcs5080219.
[36] C.K. Tagad, K.S. Rajdeo, A. Kulkarni, P. More, R. Aiyer, S. Sabharwal, Green synthesis of polysaccharide stabilized gold nanoparticles: chemo catalytic and room temperature operable vapor sensing application, RSC Adv. 4 (2014) 24014–24019, https://doi.org/10.1039/C4RA02972K.
[37] I. Hammami, N.M. Alabdallah, Gold nanoparticles: synthesis properties and applications, J. King Saud Univ. Sci. 33 (2021) 101560, https://doi.org/10.1016/j.jksus.2021.101560.
[38] C. Botteon, L. Silva, G. Ccana-Ccapatinta, T. Silva, S. Ambrosio, R. Veneziani, J. Bastos, P. Marcato, Biosynthesis and characterization of gold nanoparticles using brazilian red propolis and evaluation of its antimicrobial and anticancer activities, Sci. Rep. 11 (2021) 1974, https://doi.org/10.1038/s41598-021-81281-w.
[39] S.K. Seol, D. Kim, S. Jung, Y. Hwu, Microwave synthesis of gold nanoparticles: effect of applied microwave power and solution pH, Mater. Chem. Phys. 131 (2011) 331–335, https://doi.org/10.1016/j.matchemphys.2011.09.050.
[40] M.S. Punnoose, D. Bijimol, B. Mathew, Microwave assisted green synthesis of gold nanoparticles for catalytic degradation of environmental pollutants, Environ. Nanotechnol. Monit. Manag. 16 (2021) 100525, https://doi.org/10.1016/j.enmm.2021.100525.
[41] H.R. de Barros, L. Piovan, G.L. Sassaki, D. de Araujo Sabry, N. Mattoso, A.M. Nunes, M.R. Meneghetti, I.C. Riegel-Vidotti, Surface interactions of gold nanorods and polysaccharides: from clusters to individual nanoparticles, Carbohydr. Polym. 152 (2016) 479–486, https://doi.org/10.1016/j.carbpol.2016.07.018.
[42] R. Lotfollahzadeh, M. Yari, S. Sedaghat, A.S. Delbari, Biosynthesis and characterization of silver nanoparticles for the removal of amoxicillin from aqueous solutions using *Oenothera biennis* water extract, J. Nanostructure Chem. 11 (2021) 693–706, https://doi.org/10.1007/s40097-021-00393-x.
[43] D.K. Nguyen, C. H Jang, Ultrasensitive colorimetric detection of amoxicillin based on Tris-HCl-induced aggregation of gold nanoparticles, Anal. Biochem. 645 (2022) 114634, https://doi.org/10.1016/j.ab.2022.114634.
[44] L. Shen, J. Chen, N. Li, P. He, Z. Li, Rapid colorimetric sensing of tetracycline antibiotics with in situ growth of gold nanoparticles, Anal. Chim. Acta 839 (2014) 83–90, https://doi.org/10.1016/j.aca.2014.05.021.